

Using “Predictor Antennas” for Long-Range Prediction of Fast Fading for Moving Relays

Mikael Sternad, Michael Grieger, Rikke Apelfröjd, Tommy Svensson,
Daniel Aronsson and Ana Belén Martínez

Abstract—Channel state information at transmitters is important for advanced transmission schemes. However, feedback and transmission control delays of multiple milliseconds in LTE systems result in severe outdated of this information at vehicular velocities. Channel prediction based on extrapolation of the short-term fading is inadequate in LTE systems at vehicular velocities and high carrier frequencies.

We here propose and evaluate a simple scheme which may extend the prediction horizon when used on vehicles: Use an additional antenna, a “predictor antenna”, placed in front of the transmission antennas in the direction of travel. This is of particular interest for use with moving relays: Local access points placed on e.g. buses or trams. A measurement-based study for 20 MHz downlink channels at 2.68 GHz is reported here for both line-of-sight and non-line-of-sight conditions.

I. INTRODUCTION

Advanced wireless systems need accurate channel state information at the transmitters (CSIT) to facilitate link adaptation, beamforming, multi-user scheduling and in the future also coordinated multipoint transmission. However, channel measurements are outdated at the time of data transmission, due to various delays in the transmission control loop. This is a major problem for terminals at vehicular velocities.

The use of channel predictions can improve the situation. The short-term fading can be predicted from past and present noisy channel measurements using the fading statistics over time and frequency. This provides adequate accuracy for a prediction range in space corresponding to 0.1-0.3 carrier wavelengths, but can rarely offer useful predictions for longer distances. See e.g [1], [2] for early results on narrowband channels and [3] for a survey of results. The recent study [4] uses the best linear (Kalman) predictors on wideband OFDM systems and has confirmed these conclusions.

Prediction 0.1-0.3 wavelengths ahead would be adequate at vehicular velocities if transmission control loops had very low latency (1-2 ms) [5], [6], such as in the 4G system proposals investigated by the EU WINNER projects [7].

M. Sternad, (corresponding author) R. Apelfröjd and D. Aronsson are with Signals and Systems, Dept. of Engineering Sciences, Uppsala University, Box 534, SE-751 21 Uppsala, Sweden.

{ms,riab}@signal.uu.se,daniel.at.aronsson@gmail.com
M. Grieger and A. Belén Martínez are with the Vodafone Chair Mobile Communications Systems, Technische Universität Dresden.

{michael.grieger,anab.martinez}@ifn.et.tu-dresden.de
T. Svensson is with the Dept. of Signals and Systems, Communication Systems Group, Chalmers University of Technology, SE-41296, Gothenburg, Sweden. {tommy.svensson}@chalmers.se.

Acknowledgements: This work has received funding from the European Commissions program FP7-ICT-2009 under grant of arrangement no 247223 also referred to as ARTIST4G. We are grateful for the support of Sven-Einar Breuer, Eckhard Ohlmer and Gerhard P. Fettweis.

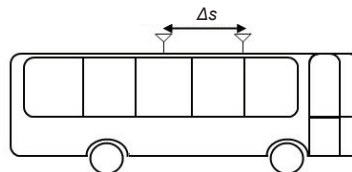


Fig. 1: The predictor antenna concept.

Present LTE systems have higher delays of at least 5 ms. Prediction horizons of 0.1-0.3 wavelengths are here adequate at pedestrian velocities, but inadequate for vehicular velocities at carrier frequencies above one GHz.

Vehicles such as trams or buses are of interest since they constitute natural hot-spots. Local access points, *moving relay nodes*, could be placed inside such vehicles, with short propagation distances and good channels to all users on the vehicle [8]. The access points then connect to the fixed network via relay links (“backhaul links” in 3GPP terminology), with antennas mounted outside of the vehicle. The relay links would become bottlenecks of the transmission scheme. Improving their performance and reliability is important to the success of the concept of moving relay nodes.

This vehicular scenario provides an opportunity as well as a challenge: The vehicle velocity and direction is relatively constant over the required 5 ms prediction horizon. Predictions could then be obtained by an antenna located some distance directly in front of the antennas used for transmission. This “*predictor antenna*” might be the first antenna of a linear antenna array or a separate antenna.

In this paper, we investigate the predictability of complex channel gains for 20 MHz channels in 2.68 GHz downlinks, as a function of the antenna separation. Measurement data are used to obtain a realistic assessment. To our knowledge, the only similar previous investigation was performed by R.G. Vaughan and co-workers in 1991 for narrowband channels at 851 MHz [10]. That paper reported high correlation of the signal envelopes between the time-delayed channel measured at one antenna and the channel measured at another antenna behind it, both placed on the roof of a vehicle. The correlation remained high for distances up to several wavelengths. However, a large reduction of correlations was measured for antenna separations of 0.2-0.4 wavelengths, due to mutual electromagnetic coupling effects [11]. (The main interest of this work was to what extent correlation is low, to obtain diversity. Here, a high correlation is useful.)

Below, we introduce the concept of moving relay nodes and their relay link antennas in Section II. Channel prediction

accuracy results for the short term-fading of radio channels are reviewed in Section III and the predictor antenna is introduced. The experimental investigation follows in Section IV.

II. MOVING RELAY NODES

The present work is related to an ongoing comparative study on how to best serve data hungry users on moving vehicles, such as buses and trams, in metropolitan areas [8].

Concentrations of vehicle-borne users inside buses and trams constitute natural hot-spots. However, their transmissions are subject to penetration losses through vehicle windows and suffer from fast fading. A potential remedy to these problems is to equip the vehicle with internal short-range transceivers and a sophisticated transceiver for the relay link to the fixed network. More efficient technology can then be used for the relay link, to increase its capacity.

It is therefore of interest to study Layer 2 or 3 relays installed on vehicles, with outdoor antennas for the relay backhaul link and indoor antennas for transmissions to/from users. Preliminary investigations show that substantial spectral efficiency gains are possible [9].

To enable the use of CSIT over the relay link, predictions of the complex channel gains would be required for a broadband frequency-selective fading channel. The predictions are required for a prediction horizon that corresponds to the delay of the transmission control loop, including channel prediction, feedback, scheduling, and precoding. These delays may differ for uplinks and downlinks and for FDD versus TDD, but are expected to be at least 5 ms in present and near-future releases of the LTE standard.

III. PREDICTION OF SHORT-TERM FADING

A prediction horizon of L seconds is equivalent to prediction over space expressed in terms of carrier wavelengths:

$$Lf_d = \frac{Lv}{\lambda} = \frac{Lv f_c}{c_0} \quad [\text{wavelengths}], \quad (1)$$

where f_d is the maximal Doppler frequency in Hz, v is the vehicle velocity in m/s, λ is the carrier wavelength in m, c_0 is the velocity of light and f_c is the carrier frequency. The relation is illustrated by Fig. 2 for $L = 5$ ms. For example, the prediction range at $f_c = 2.68$ GHz is 0.62λ at $v = 13.88$ m/s (50 km/h) and 1.24λ at $v = 27.77$ m/s (100 km/h). At the pedestrian velocity 5 km/h, it is only 0.062λ .

A. Prediction Based on Past Samples

The short-term fading can be predicted from noisy past channel estimates. For adaptive transmit beamforming, both the channel gain and the phase are needed, so the complex channel has to be predicted, not only its power.¹ For frequency-selective fading broadband channels, the most powerful linear prediction of complex channel gains is obtained by Kalman predictors [4]. In FDD systems, such predictors are preferably implemented at the receiver side.

¹This is advantageous also in cases when only the power is of interest for e.g. link adaptation [12]. A much higher prediction accuracy is then obtained by predicting the complex channel and then calculating the power prediction from it, as compared to predicting power from past power samples [1], [2].

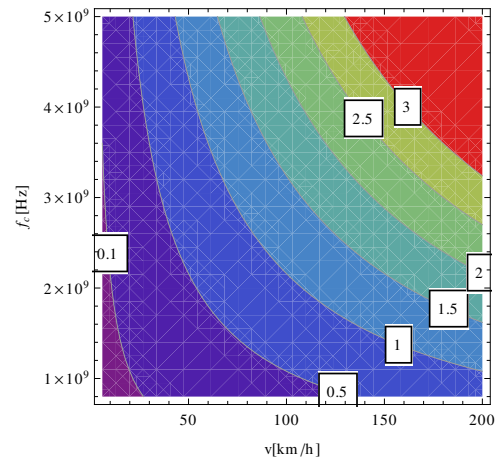


Fig. 2: Required prediction range expressed in carrier wavelengths corresponding to a prediction horizon of 5 ms, as a function of the vehicle velocity and the carrier frequency.

The predictors utilize known reference signals and estimated models of the fading statistics over time and frequency.

Fig. 3 and Fig. 4 below are from Chapter 6 of [4]. They indicate typical Kalman predictor performances as a function of the prediction range, expressed as the normalized mean square prediction error (NMSE) of time-varying complex OFDM channel coefficients $h(t)$,

$$\text{NMSE} = \frac{E|h(t_0 + L) - \hat{h}(t_0 + L|t_0)|^2}{\sigma_h^2}, \quad (2)$$

where $\hat{h}(t_0 + L|t_0)$ is a predictor based on (noisy) measurements up to time t_0 and where $\sigma_h^2 = E|h(t)|^2$.

A very important channel property that influences predictability is the Doppler spectrum. Fig. 3 illustrates results for the difficult case of a flat Doppler spectrum. Fig. 4 shows the more commonly discussed case of Clarke's Doppler spectrum, obtained for a large number of isotropically distributed local scatterers, all located in the horizontal plane. As shown, the performance is also affected by the SNR.²

A conclusion from our previous experience with link adaptation and scheduling is that only minor performance degradation and loss of multiuser scheduling gains result when the NMSE is less than 0.15 (around -8 dB) [5], [6]. Larger NMSE values result in significant performance losses. In the situations illustrated by Fig. 3 and Fig. 4, an NMSE of -8 dB or better is obtained for prediction horizons 0.1-0.3

²Results in these figures were calculated (not simulated) from the statistics of the Kalman predictor. The detailed assumptions differ from our considered case, but we believe the results to have general validity. The figures assume the use of the OFDM uplink of the WINNER system concept FDD mode [13]. In resource blocks of 8 subcarriers by 12 OFDM symbols = 312.5 kHz by 345.6 μ s, the first OFDM symbol of each resource block is assumed to consist only of uplink reference signals. Sets of Kalman predictors are used in the frequency domain, each filter predicting 8 subcarriers (one resource block width) in parallel. Four terminals are predicted by each Kalman predictor. Uplink reference signal patterns from different terminals are orthogonal over 8 subcarriers. NMSE results are averages over all subcarriers and terminals. All assumed vehicle velocities are 50 km/h and the carrier frequency is 3.7 GHz. The fading statistics in time is here autoregressive of order 4, and exactly known.

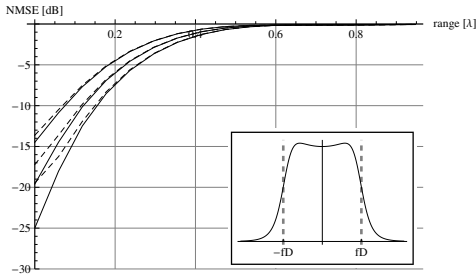


Fig. 3: Normalized mean square prediction error (NMSE) of the complex channel gain, in dB, versus the prediction horizon expressed in carrier wavelengths for non-line-of sight propagation with a flat Doppler spectrum. The curves correspond, in pairs, to SNR levels of 6, 12, and 18 dB, respectively. In each pair the dashed and solid curves show the NMSE performance for frequency selective and flat fading channels, respectively.

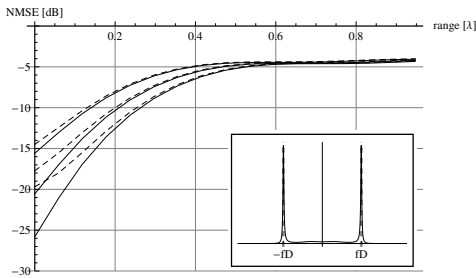


Fig. 4: Prediction performance for Clarke's Doppler spectrum, approximated by a stable autoregressive process of order 4. Assumptions and plots otherwise as in Fig. 3.

wavelengths at reasonable SNR levels. It is hard to obtain this performance at longer prediction ranges.

B. The Predictor Antenna

Channel prediction is a hard problem, but additional measurements may be of help. The electromagnetic field forms a standing wave pattern, and the vehicle moves through this pattern. If we place a second antenna in front of the one of interest, it would sample the wavefield. Its estimated channel could be used as predictor for the channel to be experienced by the rearward antenna when it reaches this position.

We here investigate a simple case with two antennas on a vehicle roof. The channels constitute time-varying complex scalar gains for OFDM subcarriers. The measured front antenna channel, $h_p(t)$, acts as predictor for the channel $h(t)$ at the rearward antenna. The predictor considered here is just a scaled and appropriately delayed filter estimate of h_p :

$$\hat{h}(t_0 + L|t_0) = a\hat{h}_p(t_0 - \Delta t + L|t_0 - \Delta t + L). \quad (3)$$

Here, a is a complex-valued scalar gain, L is the required prediction horizon, $\Delta t = \Delta s/v(t)$, where Δs is the antenna separation and $v(t)$ is the vehicle velocity. Prediction horizons $L \leq \Delta t$ can be accommodated. Since filter estimates are much more accurate than predictions (see the NMSE values in Fig. 3 and Fig. 4 for prediction range zero), this could provide significant performance gains. A smoothing estimate $\hat{h}_p(t_0 - \Delta t + L|t_0)$ could be used in (3) to increase performance at the price of higher computational complexity.

A predictor antenna does not have to be used only for prediction. On vehicles, we might use a linear antenna array with antennas placed in the forward-backward direction (with boresight direction sideways). Each antenna of the array could act as predictor for the ones behind it. (The prediction direction would be reversed when moving backwards.) One extra antenna element could be placed in front of the array, at a distance related to the maximal vehicle velocity.

Several effects may potentially reduce the prediction accuracy. One is mutual electromagnetic coupling of the antennas. Another is the influence of the moving vehicle on the standing wave pattern: It will to some extent decorrelate the field. Furthermore, the antennas are not located at the same position on the vehicle roof and may be differently affected by Fresnel diffraction at the edges of the roof. Experimental investigations of the performance are therefore required.

C. Performance Metrics and Predictor Design

The potential prediction performance will be evaluated in terms of the maximum of the correlation function between $h(t)$ and a delayed predictor antenna channel $h_p(t - \tau)$ at the same OFDM subcarrier

$$C(\tau) = E[h(t)h_p^*(t - \tau)]. \quad (4)$$

The correlation maximum should be at $\tau = \Delta t = \Delta s/v(t)$.

We model $h_p(t - \Delta t)$ as the sum of two components: A scaled $h(t)$ and a component $\tilde{h}(t)$ uncorrelated to $h(t)$:

$$h_p(t - \Delta t) = ch(t) + \tilde{h}(t), \quad (5)$$

where c is a complex scalar, $E|\tilde{h}(t)|^2 = \sigma_{\tilde{h}}^2$ and $E[h(t)\tilde{h}^*(t)] = 0$. Then, by (4) and (5),

$$C(\Delta t) = E[h(t)(c^*h^*(t) + \tilde{h}^*(t))] = c^*\sigma_h^2, \quad (6)$$

so $|c|$ represents the normalized maximal magnitude of the cross-correlation between the complex channel gains as measured at the two antennas.

Assume the receiver gains to be calibrated such that the powers of the signals received by the two antennas to be equal, so $E|h_p(t)|^2 = E|h(t)|^2 = \sigma_h^2$.

By (5), this then implies $\sigma_h^2 = |c|^2\sigma_h^2 + \sigma_{\tilde{h}}^2$, so

$$|c|^2 = 1 - \frac{\sigma_{\tilde{h}}^2}{\sigma_h^2}. \quad (7)$$

We can now relate the attainable prediction NMSE (2) to the maximal correlation by (6). Assuming $\hat{h}_p = h_p$, use of the predictor (3) with $t = t_0 + L$ and use of model (5) gives

$$\text{NMSE} = \frac{E|h(t) - a(ch(t) + \tilde{h}(t))|^2}{\sigma_h^2} = |1 - ac|^2 + |a|^2 \frac{\sigma_{\tilde{h}}^2}{\sigma_h^2}. \quad (8)$$

This NMSE is constant for all $L \leq \Delta t$. Minimization of (8) with respect to the scalar a gives $a = c^*$. The corresponding NMSE is $1 - |c|^2 = \sigma_{\tilde{h}}^2/\sigma_h^2$.

Such an MMSE predictor antenna estimator (3) has only one scalar parameter $a = c^*$. It can be implemented using an estimate of c^* obtained by a sliding window correlation.

The predictor needs an estimate of the vehicle velocity $v(t)$, which can also be obtained from this correlation function.

To further improve performance, it is of interest to investigate predictors that utilize all antennas in an antenna array as predictor antennas for each other, in combination with the use of past samples. A Kalman prediction framework is well suited for this purpose. In our present two-antenna case, let $\hat{h}_k(t_0 + L|t_0)$ denote a Kalman-based prediction based on past samples from the rear antenna up to t_0 , with variance σ_k^2 . Let $\hat{h}_a(t_0 + L|t_0)$ denote the estimate (3) from the predictor antenna, with variance σ_a^2 . When $a = c^*$ in (3), σ_a^2 is minimized and equals $\sigma_a^2 = \sigma_h^2 \text{NMSE} = \sigma_h^2(1 - |c|^2) = \sigma_h^2$.

If the errors of the two estimates are uncorrelated, the MMSE-optimal combined estimate is then given by

$$\hat{h}(t_0 + L|t_0) = \frac{1}{\sigma_k^{-2} + \sigma_a^{-2}} \left(\frac{1}{\sigma_k^2} \hat{h}_k(t_0 + L|t_0) + \frac{1}{\sigma_a^2} \hat{h}_a(t_0 + L|t_0) \right) \quad (9)$$

IV. EXPERIMENTAL EVALUATION

A. Method and Assumptions

The transmitter and the receiver were implemented using Signation's HaLo prototyping equipment. A 20 MHz OFDM signal with 2048 subcarriers was generated and up-converted to 2.68 GHz at the transmitter. Each OFDM symbol was modulated by the same Zadoff-Chu pilot sequence which features constant amplitude in the frequency domain and a low peak-to-average power ratio in the time domain. No prefix was added since the time domain signal is cyclic and the OFDM symbol duration was therefore ≈ 0.1 ms. At the receiver, snapshots of the digital base band signal received were stored after adjustable amplification (to optimize the dynamic range of an analogue-digital converter), down-conversion, analogue-digital conversion, sample rate conversion, and filtering. All other receiver algorithms such as synchronization, carrier frequency offset compensation, and FFT were applied offline. The channel was then estimated in the frequency domain.

The prototype equipment was subject to hardware impairments that could only be rectified partially. Examples are gain imbalances on different transmit/receiver paths and asynchronous local oscillators that cause effects like carrier frequency offsets, sampling clock offset, and phase noise. Thus, a compound channel (similar to a system used in the real world) including hardware effects, antenna effects, and the wireless channel was measured.

The measurement setup consisted of a single antenna transmitter located on the rooftop of an apartment at a height of about 55 m and a receiver which is connected to two standard vertically polarized dipole receive antennas (KATHREIN 80010431). The receive antennas were placed in line with variable distance Δs on the roof of a measurement bus such that the channel observed at the first (predictor) antenna could be used for predicting the channel of the antenna behind it, as previously described. At the transmitter, the $+45^\circ$ polarization of a standard cross polarized base station antenna (KATHREIN 80010541 - characterized by 58° horizontal beamwidth and 18 dBi gain)

was used. The total transmit power was 36 dBm, and with a downtilt of 9° .

Measurements were performed at a vehicular velocity of 45-50 km/h in a residential neighborhood surrounded by buildings of height 10 – 50 m. In the experiments, very low power was received at some subcarriers (including the central subcarrier). These subcarriers were excluded from the investigation which utilized 1784 out of 2048 subcarriers.

Measured data was collected by full-band measurements with duration of 200 ms at a location with line-of-sight (LOS) propagation to the base station and at a non-line of sight (NLOS) location where the base station was blocked by a building. The 200 ms windows correspond to distances of 2.78 m (≈ 24 carrier wavelengths) traveled at 50 km/h.

Distances between the two antennas were set to $\lambda/4, \lambda/2, \lambda, 2\lambda$ and 3λ . Three measurements were performed at each location for each setting of antenna distance. The exact vehicle position differed by a couple of meters between the three repetitions of each case.

B. Results

As a characterization of the propagation environment, Fig. 5 shows the Doppler spectra measured in the three experiments performed for antenna separation $\Delta s = \lambda$ at the non-line-of-sight test location. It confirms that the propagation is indeed non-line of sight, with dominating contributions from reflectors/scatterers at the side of the road. (With a velocity of 45-50 km/h, the maximal Doppler frequency f_d that would be obtained by reflectors in the direction of travel, is approximately 115 Hz.)

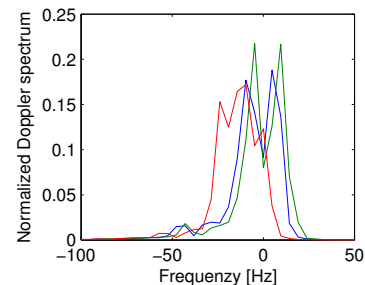


Fig. 5: Examples of Doppler spectra measured at the non-line-of sight test location by the predictor antenna.

The properties of the cross correlation functions (4) were investigated. Fig 6 exemplifies the normalized sample cross-correlations at one selected subcarrier for the three trials at the non-line-of sight test location. Results are shown for antenna separations $\Delta s \approx \lambda/4, \lambda/2$ and 2λ . For this and other subcarriers, the delay location of the peaks correspond well to the value $\Delta t = \Delta s/v$ expected for $v \approx 13$ m/s. The peak value $|c|$ is high for short antenna separations, but is markedly lower for antenna separation 2λ .

Fig. 7 shows statistics for the peak correlation magnitude $|c|$ and the corresponding attainable NMSE $1 - |c|^2$ for all the utilized subcarriers at all three trials, for the non-line-of-sight locations and locations with line-of-sight. Shown are arithmetic averages, 95th percentiles and 5th percentiles.

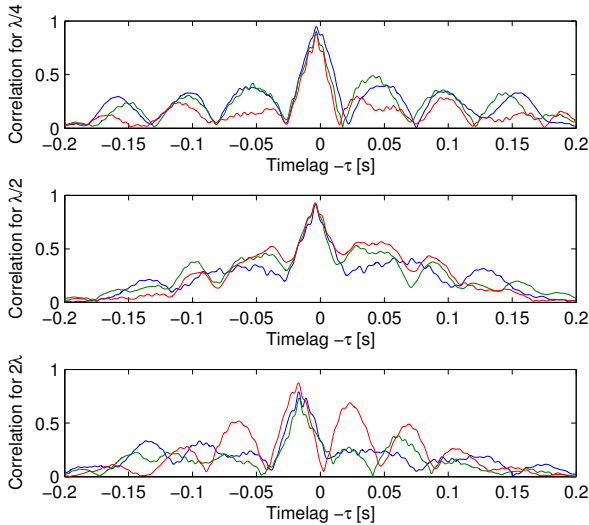


Fig. 6: Normalized cross-correlation magnitudes $|C(\tau)|$ between antenna signals at one subcarrier, for all three trials at the non-line-of-sight test location. Results are for subcarrier 800 out of 2048 and for antenna separations $\approx \lambda/4, \lambda/2$ and 2λ .

As expected, the peak correlation (and thus predictability) over a horizon $\Delta t = \Delta s/v$ is higher with line-of-sight, for all antenna separations. High correlation indicating a good NMSE (around $|c| = 0.9$ or higher) is obtained on average up to antenna separations somewhat below $\lambda/2$ in non-line-of-sight and for separations λ for the line-of-sight situations. (The peak envelope correlation $E[|h(t)||h_p^*(t - \Delta t)|]$ shows larger values, similar to those reported in [10].)

There is a significant variability of the results for different subcarriers, as indicated by the percentile values so a significant spread in predictability can be expected. (A large spread of results is observed also in prediction experiments based on previous noisy time samples. See e.g. the statistics obtained by linear prediction in Section 6.7.2 of [2].)

A significant decorrelation was observed at larger antenna separations, in particular in the non-line-of-sight case. The cause of this decorrelation is likely to be a combined effect of a disturbance of the wavefield by the moving vehicle itself and effects of differing placements of the antennas on the vehicle roof. These effects, and possible means to reduce them, need to be investigated in follow-on experiments. No decorrelation due to mutual antenna couplings at short antenna separations, as reported in [10], could be observed at $\lambda/4$ separation in the non-line-of-sight experiments. Only a weak effect was present in the line-of-sight measurements.

V. CONCLUSIONS

The results indicate that a simple predictor that uses delayed channel estimates from a predictor antenna can provide useful accuracy, on average, for prediction ranges somewhat below $\lambda/2$ in non-line-of-sight and for one wavelength for the investigated line-of-sight case. This corresponds to prediction horizons that would be required in LTE relay links for buses and trams. Investigation of

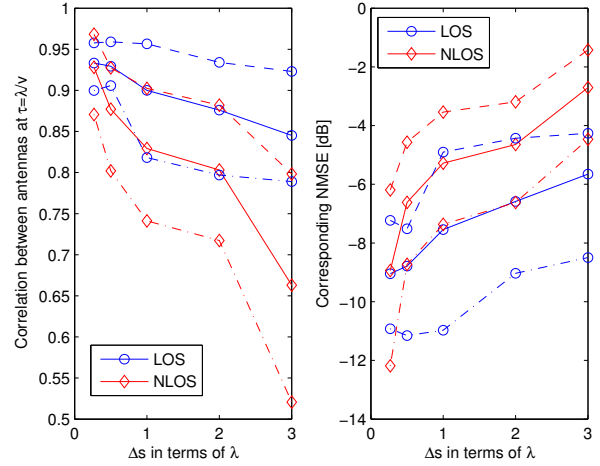


Fig. 7: Measured statistics for the peak correlation magnitude $|c|$ (left) and the corresponding attainable NMSE $1 - |c|^2$ (right). Solid: average over all subcarriers as a function of the distance between the antennas. Results for line-of-sight (rings, blue) and non-line-of-sight locations (diamonds, red). Dashed and dash-dotted lines represent the 95th and 5th percentiles, respectively.

channel predictors based on this data set are ongoing.

REFERENCES

- [1] T. Ekman, A. Ahlén and M. Sternad, "Unbiased power prediction on Rayleigh fading channels," *IEEE Vehicular Techn. Conf. VTC2002-Fall*, Vancouver, Canada, Sept. 2002.
- [2] T. Ekman, *Prediction of Mobile Radio Channels: Modeling and Design*. Ph.D. Thesis, Signals and Systems, Uppsala Univ., 2002. Available: www.signal.uu.se/Publications/pdf/a023.pdf
- [3] A. Duel-Hallen, "Fading channel prediction for mobile radio adaptive transmission systems," *Proc. of the IEEE*, vol. 95, no. 12, pp. 2299-2313, Dec. 2007.
- [4] D. Aronsson, *Channel Estimation and Prediction for MIMO OFDM Systems - Key Design and Performance Aspects of Kalman-based Algorithms*. Ph.D. Thesis, Signals and Systems, Uppsala University, March 2011. www.signal.uu.se/Publications/pdf/a112.pdf
- [5] M. Sternad, S. Falahati, T. Svensson and D. Aronsson, "Adaptive TDMA/OFDMA for wide-area coverage and vehicular velocities," *IST Summit*, Dresden, June 19-23, 2005.
- [6] Sternad, M, T. Svensson, T. Ottosson, A. Ahlén, A. Svensson and A. Brunstrom, "Towards systems beyond 3G based on adaptive OFDMA transmission," *Proceedings of the IEEE*, vol. 95, no. 12, pp. 2432-2455, Dec. 2007.
- [7] M. Döttling, A. Osseiran and W. Mohr ed., *Advanced Radio Technologies and Concepts for IMT-Advanced* Wiley, 2009.
- [8] Y. Sui, A. Papadogiannis, and T. Svensson, "The potential of moving relays - A performance analysis," *IEEE Vehicular Technology Conference VTC 2012-Spring*, Yokohama, May 2012.
- [9] Artist4G, Deliverable D3.4, "Relay configurations". July 2011. Available at <https://ict-artist4g.eu/projet/deliverables>
- [10] R.G. Vaughan, N.L. Scott and J. Southon, "Characterization of standing wave movements by in-line antennas," *IEEE Antennas and Propagation Society Symp.*, pp. 974-977, June 1991.
- [11] R.G. Vaughan and N.L. Scott, "Closely spaced terminated monopoles for vehicular diversity antennas," *IEEE Antennas and Propagation Society Symp.*, pp. 1093-1096, 1992.
- [12] S. Falahati, A. Svensson, M. Sternad and T. Ekman, "Adaptive modulation systems for predicted wireless channels," *IEEE Trans. on Communications*, vol. 52, pp. 307-316, Feb. 2004.
- [13] IST-4-027756 WINNER II, D6.13.7: Test Scenarios and Calibration Cases; Issue 2. December 2006. Available at: <http://www.signal.uu.se/Publications/wip.html>